Total and partial generalized oscillator strengths for transitions to the continuum of helium

1990 J. Phys. B: At. Mol. Opt. Phys. 23 3677

(http://iopscience.iop.org/0953-4075/23/20/025)

J. Phys. B: At. Mol. Opt. Phys. **23** (1990) 3677-3690. Printed in the UK

Total and partial generalized oscillator strengths for transitions to the continuum of helium

S M Burkov†, S I Strakhova† and T M Zajac‡

† Institute of Nuclear Physics, Moscow State University, Moscow 119899, USSR
‡ Uzhgorod State University, Uzhgorod 294000, USSR

Received 17 July 1989, in final form 7 June 1990

Abstract. The generalized oscillator strengths (GOS) for transitions to the continuum of helium between the second and third thresholds of ionization of helium by fast electrons are calculated. The total and partial GOS, the GOS ratios in the ionization of helium to the $n=1$ and $n=2$ states of the He^+ residual ion, the parameters of the autoionized states converging to the threshold $n=3$ in the total and partial GOS and the dependence of the spectroscopic characteristics of the resonances on momentum transfer are determined. The ground state of helium is described by a many-parameter wavefunction. The continuum of helium between the second and third thresholds is described with allowance for the coupling among 20 configurations, which correspond to the two-electron excitations and four configurations with the free electron above the $n=1$ and $n=2$ states of the He^+ ion.

1. Introduction

The generalized oscillator strength (GOS) for electron transitions to the continuum in the Born approximation depends only on momentum transfer and energy loss. The dependence on energy loss can show resonant structure due to the appearance of autoionizing states (AIS) of the system. The one-electron excitation of two-electron AIS is realized by electron correlations. Thus, in studying GOS, it is possible to obtain information on the structure of the continuous atomic spectrum, the applicability of different models of description of the continuum, and the AIS excitation and decay mechanism. A wide host of possibilities which arise in investigations of this type with the helium atom have already been demonstrated in the electron impact ionization of helium between the first and second ionization thresholds (60.1-65.4 eV) (Silverman and Lassettre 1964, Simpson *et al* 1965, Balashov *et al* 1972, Jacobs 1974). In these studies AIS had the single decay channel and, as a result, the ground state of the He^+ ion was populated. More recent helium photoionization experiments (Woodruff and Samson 1982, Lindle *et al* 1985, 1987) measure the partial characteristics of the process, when the He^+ ion remains in the ground state or in the first excited state. The resonant structure of the partial photoionization cross section in this region (65.4-72.9 eV) is caused by the helium AIS converging to the $n=3$ threshold. Of great interest are the data on these AIS at non-zero values of momentum transfer. Experimental data on the resonance GOS in helium between the second and third ionization thresholds are missing. In what follows we present the results of theoretical calculations.

0953-4075/90/203677+14$03.50

2. Formulation

We write

$$\mathrm{He}(n_0L_0S_0)+\mathrm{e}^-(\boldsymbol{k}_0)\rightarrow \mathrm{He}^+(nl_1)+\mathrm{e}^-(\boldsymbol{k}_1)+\mathrm{e}^-(\boldsymbol{k})$$

where $\boldsymbol{k}_0$, $\boldsymbol{k}_1$ and $\boldsymbol{k}$ are the momenta of the incoming, the knocked-on and the scattered electrons. In the Born approximation the partial GOS can be represented as (for example, Robb *et al* 1975)

$$\frac{\partial f_{nl_1}(Q)}{\partial E}=\frac{E}{Q^2}\sum_{lL}\left|\langle nl_1\varepsilon l{:}\ LS_0|\sum_{j=1}^{2}\mathrm{e}^{\mathrm{i}\boldsymbol{Q}\cdot\boldsymbol{r}_j}|n_0L_0S_0\rangle\right|^2 \tag{1}$$

where $E=k_0^2-k^2$ is the energy loss; $\boldsymbol{Q}=\boldsymbol{k}_0-\boldsymbol{k}$ is the momentum transfer; $|nl_1\varepsilon l{:}\ LS_0\rangle$ denotes the helium wavefunction with total momentum L and spin S_0, and the electron with momentum l and energy ε is the field of the He^+ ion; the electron of the He^+ ion has the quantum numbers (nl_1); $|n_0L_0S_0\rangle$ denotes the ground-state wavefunction of helium. The total GOS $\partial f/\partial E$ is the sum of the partial GOS. The differential GOS for ionization are determined by the corresponding cross sections of the electron impact ionization of atoms (Bell *et al* 1973).

The formulae for calculating the GOS for transitions into the continuum were given, for example, in the papers of Jacobs (1974) and Robb *et al* (1975). The present calculations were made using the He ground-state wavefunction with 41 parameters (Tweed 1972). The sum over the total momentum of helium was restricted to the contributions of the states with $L\leqslant 3$.

3. The helium continuous spectrum model: discussion of the calculated results

3.1. Direct fast electron ionization

In the region of the helium spectrum between the second and third ionization threshold there exist four open channels for direct ionization at total momentum $L\geqslant 1$ and three channels for $L=0$ when the electron is above the ground and first excited states of the He^+ ion. The investigations of inelastic electron scattering on He^+ ions (Burke and Taylor 1969, Haysak *et al* 1982) and the helium photoionization processes (Wage *et al* 1982, Burkov *et al* 1988, Salomonson *et al* 1985) have shown that the coupling of these open channels in the continuum of helium is strong. In the fast-electron ionization problem the coupling of the ionization channels might be expected to be also strong.

In the present GOS calculations the ionized helium wavefunction was determined by the close-coupling method. To determine the K-matrix electron scattering on He^+ ions we solved a set of three integral equations for $L=0$ and a set of four equations for the other values of total momentum. The explicit form of the set of coupled equations and the relation of the K matrix with the continuum wavefunction are given, for example, by Fano and Prats (1963) and Zajac and Strakhova (1985). In solving the set of equations for the K matrix, we used as the basis wavefunctions numerical solutions of the one-channel Schrödinger equation in a screened Coulomb potential.

The calculated results, shown in figures 1 and 2, illustrate the influence of the channel coupling on the behaviour of the GOS for the direct transition to the helium continuum. They show that the coupling of open channels substantially changes the absolute magnitudes of the GOS for population of the excited 2s and 2p states of the

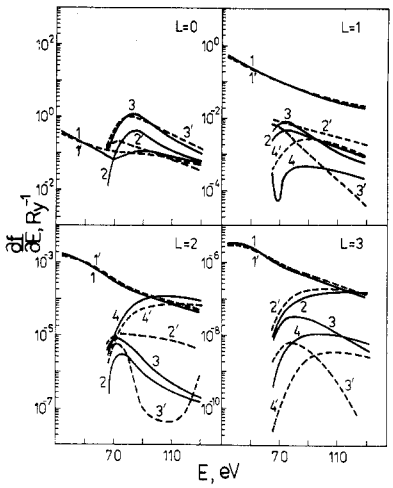

Figure 1. GOS for the direct transition to the continuum of helium as a function of energy loss at the total momentum $L=0$, 1, 2, 3; full curve, the coupling of open channels is allowed for; broken curve, the coupling of channels is neglected. Results are for momentum transfer $Q=0.1\ a_0^{-1}$. At $L=0$ curves 1 and 1′ correspond to the channel $1s\varepsilon s$; 2 and 2′, $2s\varepsilon s$; 3 and 3′, $2p\varepsilon p$. At $L\neq 0$ curves 1 and 1′ correspond to the channel $1s\varepsilon L$; 2 and 2′, $2s\varepsilon L$; 3 and 3′, $2p\varepsilon(L-1)$; 4 and 4′, $2p\varepsilon(L+1)$.

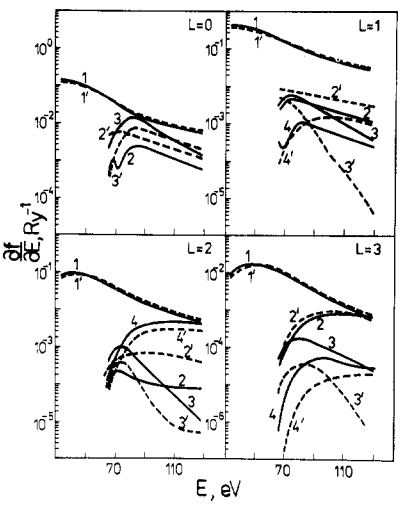

Figure 2. Same as figure 1 but for $Q=1\ a_0^{-1}$.

He^+ ion. As for the channel $1s\varepsilon L$, the relevant GOS above the second threshold are changed weakly when ionization channels for leaving He^+ in the excited states are allowed for.

At $Q=0.1\ a_0^{-1}$ (figure 1), when $L=0$, the contribution to the $n=2$ state of the residual ion above the hydrogenic $n=2$ threshold is larger than the contribution of the partial GOS for transitions to the $n=1$ state of the He^+ ion. A similar situation is also observed for $L=2$ (channel $2s\varepsilon d$) at energy loss $E>90$ eV.

At $L=1$ allowing for channel coupling the GOS curves for transitions to the $2s\varepsilon p$ channel (curve 2′) and to the $2p\varepsilon s$ channel (curve 4′) approach each other closely, as

compared with the calculations neglecting coupling (curves 2 and 4). In the 2pεd channel (curves 4 and 4′) allowance for coupling leads to a shape resonance, but the contribution of this channel to the total GOS remains small. At $L=2$ for $Q=0.1\ a_0^{-1}$ (figure 1) the coupling of the channel 2pεf (curves 4 and 4′) with other $n=2$ channels is weaker than the coupling of the channels 2sεd and 2pεp. This is inferred from the substantial difference in absolute magnitudes between curves 2 and 3 and curves 2′ and 3′ respectively. For $L=3$ the largest contribution to the total GOS from the direct transition to the $n=2$ state of the He^+ ion is provided by the 2sεf channel (curves 2 and 2′); the coupling of this channel with other channels is small as shown by the closeness of curves 2 and 2′. The channels 2pεd (curves 3 and 3′) and 2pεg (curves 4 and 4′) are coupled strongly, though their contribution to the total GOS is much smaller compared with contributions from the 2sεf channel.

The estimates of the coupling effect, which were obtained from the analysis of the GOS for momentum transfer $Q=0.1\ a_0^{-1}$, hold true for $Q=1\ a_0^{-1}$ (figure 2). As Q increases, the relative contribution of the partial GOS for transitions to the $n=2$ state is decreasing. For example, for $L=0$ the partial GOS for transitions to the $n=1$ state of the He^+ ion (curves 1 and 1′) is larger in absolute magnitude than all the other GOS. A shape resonance arises in the 2sεs channel if coupling is allowed for (curve 2).

As for the contribution provided to the GOS by the transition of states with different L, it follows from the analysis of the data shown in figure 3 that, for small Q (for example, $Q=0.3$ or $0.5\ a_0^{-1}$), the main contribution to the total GOS is provided by the states with $L=0$ and $L=1$. The contribution of the states with $L=2$ is smaller by an order of magnitude and for $L=3$ by a factor of 10^2. In the range $Q=1.0$-$1.8\ a_0^{-1}$ the contribution provided to the total GOS by the states with $L=1$ is greater than with $L\neq 1$. For $Q=2.1$-$3.0\ a_0^{-1}$ as seen from figure 4, the contributions from states with $L=0$ and $L=1$ become comparable, and the contribution of the states D and F is much smaller. At momentum transfer $Q=4.1$-$5.5\ a_0^{-1}$ the contribution decreases with increasing L. As a result there is no reason to expect an increased contribution of the

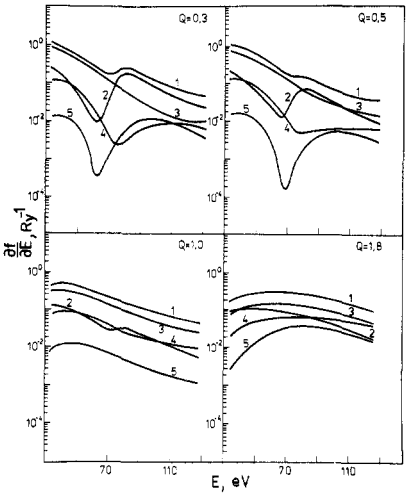

Figure 3. Contribution to the total GOS for the direct transitions to the continuum of helium (curve 1) provided by the states with $L=0$ (curve 2), $L=1$ (curve 3), $L=2$ (curve 4), $L=3$ (curve 5), as a function of energy loss E at different values of the momentum transfer $Q=0.3$-$1.8\ a_0^{-1}$.

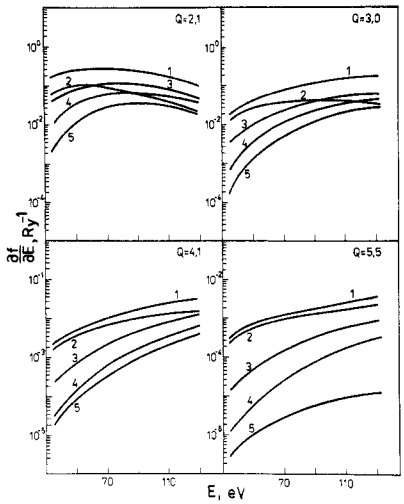

Figure 4. Same as figure 3 but for $Q = 2.1\text{-}5.5\ a_0^{-1}$.

states with $L > 3$ to the total GOS since even the $L = 3$ state gives a small contribution at all the values of the momentum transfer we are considering.

Figure 5 is a comparison between the total GOS (curve 1) and the partial differential GOS for populating the $n = 2$ state of the He^+ ion (curve 2) at $Q = 0.1\text{-}1.6\ a_0^{-1}$. It is

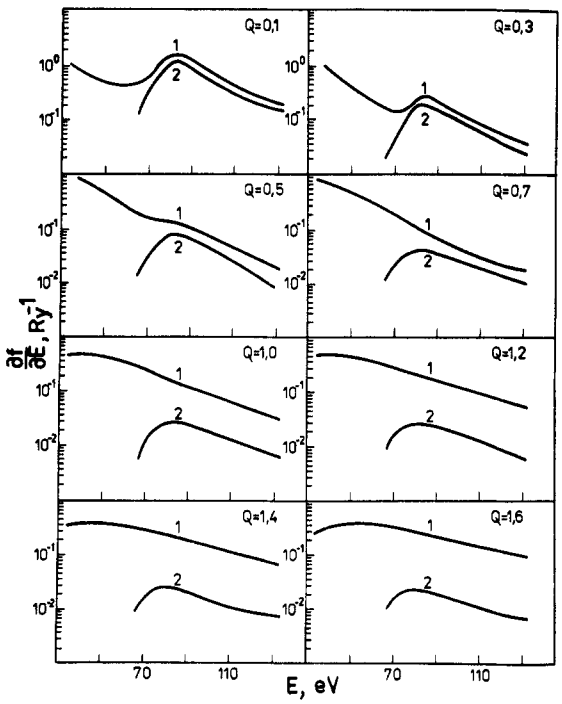

Figure 5. GOS for the direct transitions to the continuum of helium as a function of energy loss E at different values of the momentum transfer $Q = 0.1\text{-}1.6\ a_0^{-1}$. Curve 1, the total GOS. Curve 2, the partial GOS for populating the $n = 2$ state of He^+.

seen that at small momentum transfers the contribution provided by the direct transition to $n=2$ is substantial and has a great influence on the shape of curve 1. According to theory and experiment, in photoionization processes at $Q=0$ the residual He^+ ion remains with a higher probability in the $n=2$ state rather than in the $n=1$ state (Woodruff and Samson 1982, Lindle *et al* 1985, Burkov *et al* 1988). The contribution provided to the total GOS by the partial GOS for transitions to the $n=2$ state of the residual ion decreases with increasing Q when $Q \geqslant 1\ a_0^{-1}$.

At the mean values $Q=1.0$–$4.1\ a_0^{-1}$ (figures 5, 6) the He^+ residual ion remains with a higher probability in the $n=1$ state, i.e. the ratio $(\partial f_{n=2}/\partial E)/(\partial f/\partial E)$ decreases strongly. Figure 7 is a plot of the ratio $(\partial f_{n=2}/\partial E)/(\partial f_{n=1}/\partial E)$ against energy loss. Analysis of the data shown in figure 7 leads us to the conclusion that at $Q=0.1\ a_0^{-1}$ the ratio of the partial GOS varies between 0.5 and 10.0; at $Q=0.3\ a_0^{-1}$ in the range 0.12–2.0; at $Q=0.5\ a_0^{-1}$ between 0.07 and 1.2. As Q increases further the interval becomes more narrow, and at $Q=2.5\ a_0^{-1}$ it begins to get a little wider, and at $Q=5\ a_0^{-1}$ the ratio varies between 0.08 and 0.14.

3.2. Resonance ionization of helium between the second and third thresholds

The GOS for transitions in the region of the helium continuum above the hydrogenic $n=2$ threshold will behave non-monotonically due to the appearance of AIS converging to the $n=3$ threshold of the He atom. In the expansion of the helium continuum we included a finite number of basis configurations corresponding to two-electron states (closed channels) and to one free electron above the ground and first excited states

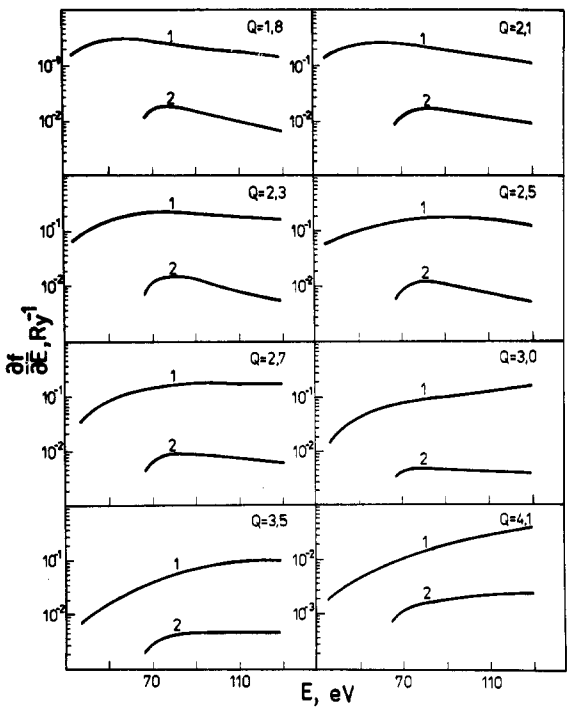

Figure 6. Same as figure 5 but for $Q=1.8$–$4.1\ a_0^{-1}$.

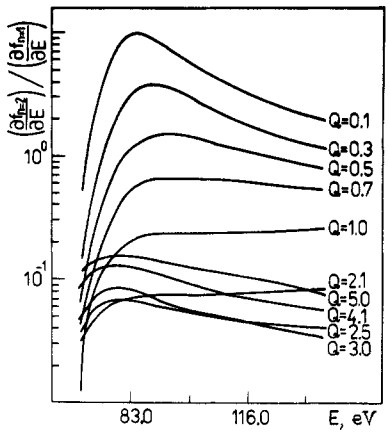

Figure 7. Ratio of the partial differential GOS for the direct transitions $(\partial f_{n=2}/\partial E)/(\partial f_{n=1}/\partial E)$ in helium at different Q as a function of energy loss.

of the He^+ ion (open channels). The calculations included the states with the total momentum of helium $L \leqslant 3$.

The subspace of open channels contains three configurations for $L=0$ and four configurations for the other L values, which correspond to the inclusion of the channels $1s\varepsilon L$, $2s\varepsilon L$, $2p\varepsilon(L-1)$, $2p\varepsilon(L+1)$ in the calculations; for each angular momentum L the subspace of closed channels contained 20 configurations of type $3ln'l'\,^1L$ with $l=0$, 1 and 2; Coulomb functions with charge $Z=2$ were used as basis functions. The submatrix associated with the subset $|3ln'l'\,^1L\rangle$ of states is diagonalized as zeroth approximation. To continue the procedure after such a simplification is justified, because it is accepted that the off-diagonal elements in the closed-channel submatrix contribute negligibly to the total energy matrix.

The subspace of open channels was also pre-diagonalised. The procedure of partial pre-diagonalization of open channels (Fano and Prats 1963) is equivalent in the present case to determination of the wavefunction of the electron in the He^+ ion field with allowance for the close coupling of the channels of the non-resonance inelastic scattering. Thus, the solution of the set of coupled integral equations for the K matrix of electron scattering on the He^+ ion was used as the wavefunctions of the pre-diagonalized subspace of open channels.

In order to allow for the interaction between the pre-diagonalized subspaces of open and closed channels, we used the method of configuration interaction in the complex number representation (Burkov *et al* 1988). The general solution of the set of equations (Fano 1961) was written so that the complex continuum wavefunction in the region of the AIS had T-matrix asymptotics (see equation (4) of Burkov *et al* 1988). Fano (1961) used K-matrix asymptotics in the real number representation (see equation (48) of Fano 1961). In our approach the positions and the widths of resonances are calculated as real and imaginary parts of eigenvalues of the Hamiltonian complex matrix which describes the interaction of configurations of the pre-diagonalized closed channels through the pre-diagonalized open channels at the off- and on-shell points. The energy dependence of the eigenvalues of the complex matrix in the excitation energy region in question is weak and, therefore, in the case of many resonances it is also possible to introduce the characteristics of separate AIS positions E_r, widths Γ and line-shape parameters q in the total and partial GOS, just as in the paper of Fano

(1961) for the case of one resonance. In the present calculations the characteristics of the AIS can be introduced no matter whether this resonance is isolated in the cross sections or contributes to the envelope of a few coupled closely spaced resonances. The formulae used in this approach for the resonance photoionization of helium between the second and third thresholds are given, for example, in the paper by Burkov *et al* (1988). In the present calculations using equation (1), the above-described formalism was used to determine the helium continuum wavefunction at certain values of the total angular momentum L.

The analysis of our results shows that the resonant structure caused by AIS is most pronounced in the energy dependence of the partial GOS for ionization of helium leaving He^+ in the excited $n=2$ state.

We have studied the influence of different configurational interactions on the absolute magnitudes of GOS. In variant A of our calculation we allowed for all the interactions between the configurations of open and closed channels, using the method of configuration interaction in the complex number representation. The results are shown by the full curves in figures 8 and 9 and in tables 1-4 (Sections A). If we neglect the interaction of AIS with the continuum in the diagonalization of the Hamiltonian matrix and the interaction of the AIS with the continuum at the off-shell points in determining the wavefunctions in the formalism of Burkov *et al* (1988), we arrive at the diagonalization approximation, which was introduced in the papers of Balashov *et al* (1970) and Haysak *et al* (1982). This approximation was used by Balashov *et al* (1972, 1973) to solve the problem of ionization of helium by fast electrons below the second ionization threshold. The results of our calculation in the diagonalization approximation between the second and third thresholds are shown in figures 8 and 9 and in sections B of tables 1-4. The positions of resonances calculated in the diagonalization approximation differ slightly from those calculated in variant A, which leads to a rightwards shift of the broken curves in figure 8.

In variant A1, as compared with case A, we neglected the interaction of AIS through the continuum at the off-shell points. The results are given in figure 9 (the broken curve) and in sections A1 of tables 1-4.

In variant B1 we neglected the interaction of AIS through the continuum at the on-shell points in diagonalising the Hamiltonian matrix but retained the interaction through the continuum at the on- and off-shell points in determining the wavefunctions in the formalism of Burkov *et al* (1988). Accordingly, the calculation in variant B1 might be expected to give results similar to those of the diagonalization calculation. This is seen from the tables and figure 9.

The interaction of AIS through the continuum is important in certain cases. Only case A shows resonant structure caused by the third (the numbering is the same as in the tables) ^1S resonance and the second ^1P and ^1F resonances at $Q=1.0\ a_0^{-1}$ and such structure due to the fourth ^1P and fourth ^1D AIS at $Q=3.0\ a_0^{-1}$.

Let us compare the GOS calculations by the method of configuration interaction in the complex number representation (figure 10) with the calculation in the diagonalization approximation (figure 11). In some cases, especially in the range 71-73 eV, one can see separate resonances in figure 10, whereas in figure 11 the corresponding curves in the same energy interval are, as a matter of fact, envelopes. This indicates that for separate resonances the interaction in the subspace of closed channels through the continuum at the off-shell points plays a significant role.

The present calculations have shown that at small values of momentum transfer the contribution of the term ^1S is dominant and the resonances of the other terms in

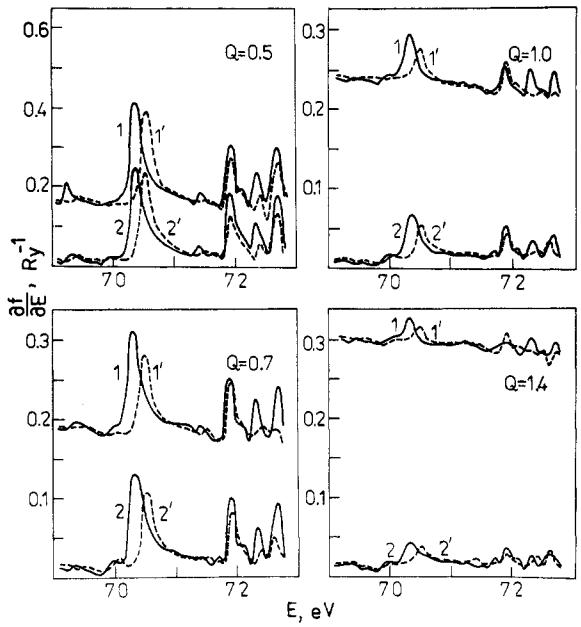

Figure 8. Resonant structure of the continuum of helium between the second and third thresholds at $Q = 0.5$-$1.4\ a_0^{-1}$. Curves 1 and 1', the total GOS; curves 2 and 2', the partial GOS for population of the $n = 2$ state of He^+; the full curves, the method of configuration interaction in the complex number representation; broken curves, the diagonalization approximation; E, energy loss.

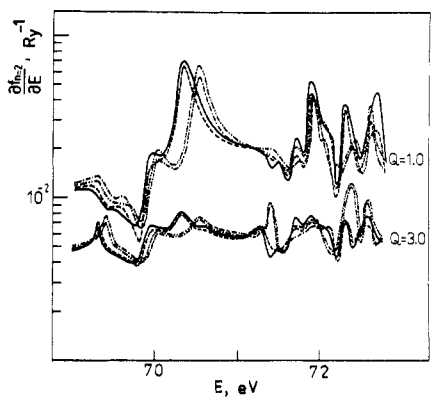

Figure 9. Resonant structure of the partial GOS for ionization of helium leaving He^+ in the $n = 2$ state at $Q = 1.0\ a_0^{-1}$ and $Q = 3.0\ a_0^{-1}$. The sum over the total momentum L includes $L = 0$, 1, 2, 3. The calculation was carried out in variant A (——); variant B (— · —); variant A1 (— —); variant B1 (— · · —). For the approximation used in the variants see the text.

Table 1. Parameters of the lowest ^{1}S AIS in He from the series of resonances converging to the threshold $n = 3$, in the total and partial GOS at the momentum transfer $Q = 0.1\ a_0^{-1}$, according to the present calculations. The variants are described in the text.

N AIS	E_r (eV)	Γ (eV)	q	ρ^2	$q_{n=2}$	$\rho^2_{n=2}$	Variant
1	69.323	0.089	5.48	0.19	6.18	0.14	A
2	70.320	0.180	4.71	0.55	4.06	0.79	
3	71.371	0.041	2.77	0.31	2.88	0.25	
4	71.860	0.046	3.66	0.78	3.26	1.00	
1	69.324	0.090	5.40	0.18	6.10	0.12	A1
2	70.308	0.185	4.65	0.52	3.92	0.77	
3	71.369	0.041	2.60	0.29	2.76	0.23	
4	71.858	0.044	3.51	0.70	3.12	0.92	
1	69.396	0.083	3.85	0.16	4.50	0.11	B
2	70.490	0.173	3.88	0.49	3.35	0.69	
3	71.401	0.041	2.24	0.29	2.33	0.23	
4	71.910	0.042	3.67	0.55	3.25	0.72	
1	69.397	0.082	4.25	0.16	4.84	0.11	B1
2	70.499	0.166	4.42	0.51	3.84	0.71	
3	70.406	0.041	2.29	0.30	2.34	0.25	
4	71.913	0.044	3.48	0.62	3.10	0.79	

Table 2. Same as table 1 but for ^{1}P AIS.

N AIS	E_r (eV)	Γ (eV)	q	ρ^2	$q_{n=2}$	$\rho^2_{n=2}$	Variant
1	69.865	0.198	0.59	0.07	0.98	0.69	A
2	71.251	0.001	13.95	10^{-4}	−1.58	0.02	
3	71.465	0.074	−1.12	0.01	−14.06	10^{-4}	
4	71.660	0.079	0.43	0.08	0.78	0.77	
1	69.855	0.199	0.33	0.07	0.74	0.72	A1
2	71.251	0.001	17.90	10^{-5}	−1.82	0.02	
3	71.463	0.067	−1.79	0.01	−3.61	0.02	
4	71.660	0.080	0.06	0.07	0.47	0.78	
1	69.918	0.176	0.38	0.07	0.78	0.70	B
2	71.242	0.001	19.63	10^{-5}	−1.71	0.02	
3	71.472	0.068	−2.08	0.01	−6.50	10^{-3}	
4	71.684	0.060	0.10	0.07	0.50	0.78	
1	69.928	0.165	0.63	0.07	1.01	0.67	B1
2	71.242	0.001	16.63	10^{-5}	−1.52	0.02	
3	71.481	0.062	−1.47	0.01	−89.30	10^{-5}	
4	71.688	0.063	0.46	0.07	0.80	0.75	

the total GOS are weak up to $Q = 1.0\ a_0^{-1}$. But at $Q = 1.5\ a_0^{-1}$ the contribution of the term ^{1}P is already larger than that of the term ^{1}S in the absolute magnitude and the ^{1}P resonances become more pronounced in the partial GOS for ionization of helium leaving He^+ in the $n = 2$ state. The lowest ^{1}D resonance is also observed only when Q becomes larger than $1.0\ a_0^{-1}$. The first ^{1}F resonance, as seen from figure 10 has a distinct profile only when $Q > 2.1\ a_0^{-1}$. In the diagonalization calculation (figure 11) its profile is much less pronounced.

Table 3. Same as table 1 but for ^{1}D resonances.

N AIS	E_r (eV)	Γ (eV)	q	ρ	$q_{n=2}$	$\rho^2_{n=2}$	Variant
1	69.694	0.150	1.40	0.02	8.4	10^{-3}	A
2	70.540	0.119	−0.42	0.04	1.65	0.16	
3	71.211	0.011	−1.80	0.24	10.71	0.11	
4	71.558	0.017	−0.03	0.29	−2.50	0.30	
1	69.685	0.150	1.31	0.02	8.32	0.01	A1
2	70.543	0.116	−0.40	0.04	1.56	0.12	
3	71.210	0.011	−1.81	0.20	10.40	0.11	
4	71.564	0.018	−0.06	0.29	−2.12	0.24	
1	69.671	0.151	−2.30	0.02	−2.15	0.14	B
2	70.504	0.122	−0.95	0.04	0.83	0.10	
3	71.225	0.011	−2.10	0.96	7.20	0.19	
4	71.550	0.214	−1.81	0.07	6.50	0.06	
1	69.685	0.151	−2.41	0.12	−2.40	0.12	B1
2	70.521	0.120	−0.92	0.04	0.89	0.12	
3	71.228	0.010	−2.11	0.80	6.80	0.17	
4	71.556	0.210	−1.72	0.07	6.00	0.05	

Table 4. Same as table 1 but for ^{1}F resonances.

N AIS	E_r (eV)	Γ (eV)	q	ρ	$q_{n=2}$	$\rho^2_{n=2}$	Variant
1	70.886	0.091	1.25	0.02	1.20	0.62	A
2	71.479	0.005	3.70	10^{-3}	2.34	0.03	
3	71.992	0.024	0.86	0.03	0.09	0.58	
4	72.135	10^{-4}	2.51	0.03	2.18	0.71	
1	70.875	0.092	1.09	0.02	1.05	0.64	A1
2	71.482	0.005	2.57	10^{-3}	2.10	0.03	
3	71.998	0.024	0.70	0.03	0.74	0.55	
4	72.135	10^{-4}	2.00	0.03	2.20	0.69	
1	70.875	0.087	1.07	0.02	1.10	0.64	B
2	71.480	0.005	2.37	10^{-3}	1.89	0.04	
3	71.992	0.025	0.68	0.03	0.73	0.59	
4	72.138	10^{-4}	3.29	0.02	2.66	0.59	
1	70.888	0.087	1.22	0.02	1.19	0.62	B1
2	71.482	0.005	2.56	10^{-3}	2.13	0.04	
3	71.994	0.023	0.84	0.02	0.86	0.57	
4	72.143	10^{-4}	3.38	0.02	2.70	0.35	

At fixed energy loss, as follows from the data shown in figures 10 and 11, the absolute magnitude of the partial GOS always decreases with increasing momentum transfer Q.

Figure 12 shows the ratio $(\partial f_{n=2}/\partial E)/(\partial f_{n=1}/\partial E)$ of the partial GOS for populating the $n=2$ and $n=1$ states of He^+ in the ionization by fast electrons. This ratio also exhibits a resonant structure. Starace (1977) was the first to report this result for the case of the resonance photoionization at $Q=0$. It is seen from figure 12 that at small

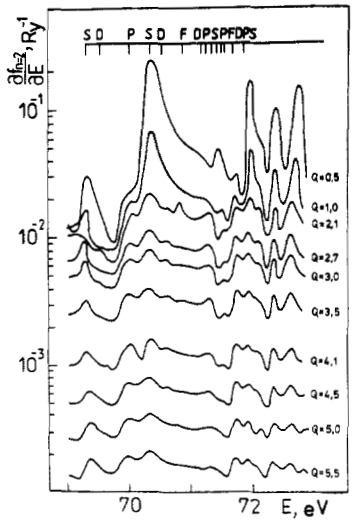

Figure 10. Partial GOS for the transition to the helium continuum (resonance process) with the population of the $n=2$ state of the He^+ ion at different Q are plotted against energy loss E. The calculated positions of the resonances are given at the top of the figure. The calculation was performed by the configuration interaction method in the complex number representation.

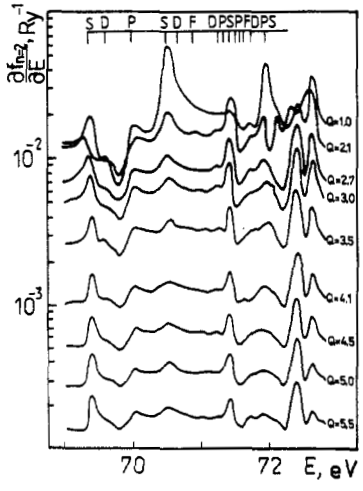

Figure 11. Same as figure 10, but the calculation was made in the diagonalization approximation.

momentum transfer, say, $Q=0.1\ a_0^{-1}$ this ratio varies between 0.2 and 12.0; at $Q=0.3\ a_0^{-1}$ between 0.15 and 0.4; at $Q=0.5\ a_0^{-1}$ between 0.1 and 1.5; at $Q=1.0\ a_0^{-1}$ between 0.04 and 0.3 and then it decreases; at $Q=3.0\ a_0^{-1}$ this ratio varies from 0.05 to 0.12. Thus, the probability that the excited $n=2$ state of the He^+ ion will be populated in the region of AIS converging to the third threshold is much larger at small values of momentum transfer.

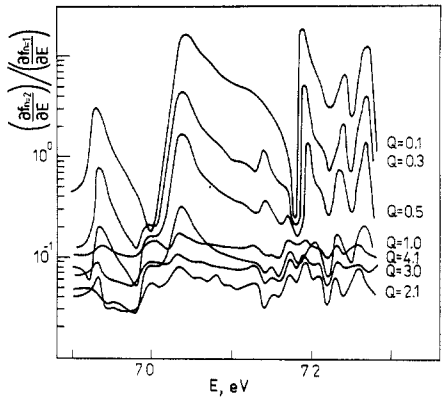

Figure 12. Ratio of the partial GOS for the resonance transition to the continuum of helium with the population of the $n = 2$, $n = 1$ states of the He^+ ion, as a function of energy loss at a few values of the momentum transfer and $Q = 0.1$-$4.1\ a_0^{-1}$.

Figure 13 illustrates the Q dependences of the lineshape parameters q, $q_{n=1}$, $q_{n=2}$ and also of the parameters ρ^2, $\rho^2_{n=1}$ and $\rho^2_{n=2}$ that were introduced by Fano (1961) and determined in the paper of Burkov *et al* (1988). The Q dependences of $q_{n=2}$ and q for the lowest ^1S and ^1F AIS have a discontinuity. The corresponding parameters $\rho^2_{n=2}$ and ρ^2 at these energy points tend to zero such that the GOS curves contain no singularities. As can be inferred from figure 13, at $Q \to 0$ the above characteristics for the ^1P lowest resonance become the same as in the case of photoionization (Woodruff and Samson 1982, Lindle *et al* 1985, 1987, Burkov *et al* 1988). As to other resonances,

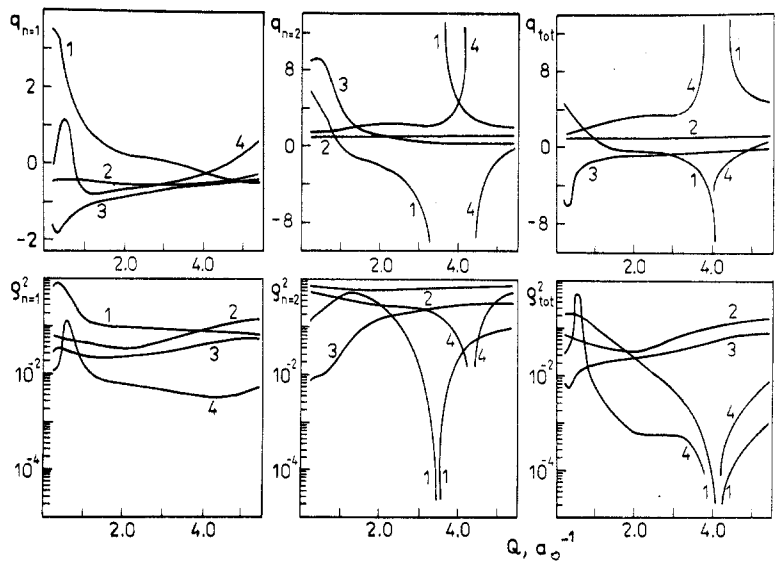

Figure 13. The lineshape parameters q and parameters ρ^2 in the total and partial ($n = 1$ and $n = 2$ states of He^+) generalized oscillator strengths for the lowest ^1S (curve 1), ^1P (curve 2), ^1D (curve 3), ^1F (curve 4) resonances, as a function of momentum transfer Q. Calculation by the method of configuration interaction in the complex number representation.

such a dependence gives us an idea of how the GOS curves shown in figures 8–11, will be transformed in going to other values of momentum transfer.

Acknowledgment

The authors are grateful to Professor V V Balashov for suggesting this problem and for helpful discussions.

References

Balashov V V, Grishanova (Strakhova) S I, Kruglova I M and Senashenko V S 1970 *Opt. Spectrosk.* **28** 859
Balashov V V, Lipovetsky S S, Pavlichenkov A V, Polyudov A N and Senashenko V S 1972 *Opt. Spectrosk.* **32** 10
Balashov V V, Lipovetsky S S and Senashenko V S 1973 *Opt. Spectrosk.* **35** 11
Bell K L, Kingston A E and Taylor I R 1973 *J. Phys. B: At. Mol. Phys.* **6** 2271
Burke P G and Taylor A J 1969 *J. Phys. B: At. Mol. Phys.* **2** 44
Burkov S M, Letyaev N A, Strakhova S I and Zajac T M 1988 *J. Phys. B: At. Mol. Opt. Phys.* **21** 1195
Fano U 1961 *Phys. Rev.* **124** 1866
Fano U and Prats F 1963 *Proc. Nat. Acad. Sci. India* A **33** 1193
Haysak M I, Lengyel V I, Navrotsky V T and Sabad E P 1982 *Ukrainsky Phys. J.* **27** 1617
Jacobs V L 1974 *Phys. Rev.* A **10** 499
Lindle D W, Ferrett T A, Becker U, Kobrin P H, Truesdale C M, Kerkhoff H G and Shirley D A 1985 *Phys. Rev.* A **31** 714
Lindle D W, Ferrett T A, Heimann P A and Shirley D A 1987 *Phys. Rev.* A **36** 2112
Robb W D, Rountree S P and Burnett T 1975 *Phys. Rev.* A **11** 1193
Salomonson S, Carter S L and Kelly H P 1985 *J. Phys. B: At. Mol. Phys.* **18** L149
Silverman S M and Lassettre E N 1964 *J. Chem. Phys.* **40** 1265
Simpson J A, Chamberlain G E and Mielzarek S R 1965 *Phys. Rev.* A **139** 1039
Starace A F 1977 *Phys. Rev.* A **16** 221
Tweed R J 1972 *J. Phys. B: At. Mol. Phys.* **5** 810
Wage A, Ivanov P B and Senashenko V S 1982 *Vestnik MGU Ser. 3* **23** (1) 49
Woodruff P R and Samson J A R 1982 *Phys. Rev.* A **25** 848
Zajac T M and Strakhova S I 1985 *Opt. Spectrosk.* **59** 17